Paleoceanography and Paleoclimatology

RESEARCH ARTICLE
10.1029/2021PA004323

Fidelity of the Coral Sr/Ca Paleothermometer Following Heat Stress in the Northern Galápagos

Anson H. Cheung[1], Julia E. Cole[2], Diane M. Thompson[3], Lael Vetter[3], Gloria Jimenez[4], and Alexander W. Tudhope[5]

[1]Department of Earth, Environmental, and Planetary Sciences, Brown University, Providence, RI, USA, [2]Department of Earth and Environmental Sciences, University of Michigan, Ann Arbor, MI, USA, [3]Department of Geosciences, University of Arizona, Tucson, AZ, USA, [4]Chubb Limited, Philadelphia, PA, USA, [5]School of Geosciences, University of Edinburgh, Edinburgh, UK

Key Points:

- We present Sr/Ca and Mg/Ca measurements of two corals from the northern Galápagos, spanning 25–30 years following the 1982-3 El Niño event
- In the faster-growing colony, the Sr/Ca-SST relationship weakens after heat stress
- Excluding data after the heat stress event from proxy calibration improves temperature reconstruction statistics

Supporting Information:

Supporting Information may be found in the online version of this article.

Correspondence to:

J. E. Cole,
colejul@umich.edu

Citation:

Cheung, A. H., Cole, J. E., Thompson, D. M., Vetter, L., Jimenez, G., & Tudhope, A. W. (2021). Fidelity of the coral Sr/Ca paleothermometer following heat stress in the northern Galápagos. *Paleoceanography and Paleoclimatology*, *36*, e2021PA004323. https://doi.org/10.1029/2021PA004323

Received 17 JUN 2021
Accepted 5 NOV 2021

Author Contributions:

Conceptualization: Anson H. Cheung, Julia E. Cole, Diane M. Thompson, Gloria Jimenez, Alexander W. Tudhope
Formal analysis: Anson H. Cheung
Funding acquisition: Julia E. Cole, Gloria Jimenez, Alexander W. Tudhope
Investigation: Anson H. Cheung, Julia E. Cole, Diane M. Thompson, Lael Vetter, Gloria Jimenez, Alexander W. Tudhope
Methodology: Anson H. Cheung, Julia E. Cole, Diane M. Thompson, Lael Vetter
Writing – original draft: Anson H. Cheung, Julia E. Cole, Diane M. Thompson
Writing – review & editing: Anson H. Cheung, Julia E. Cole, Diane M. Thompson, Lael Vetter, Gloria Jimenez, Alexander W. Tudhope

Abstract Coral Sr/Ca records have been widely used to reconstruct and understand past sea surface temperature (SST) variability in the tropical Pacific. However, in the eastern equatorial Pacific, coral growth conditions are marginal, and strong El Niño events have led to high mortality, limiting opportunities for coral Sr/Ca-based SST reconstructions. In this study, we present two ~25-year Sr/Ca and Mg/Ca records measured on modern *Porites lobata* from Wolf and Darwin Islands in the northern Galápagos. In these records, we confirm the well-established relationship between Sr/Ca and SST and investigate the impact of heat stress on this relationship. We demonstrate a weakened relationship between Sr/Ca and SST after a major (Degree Heating Months 9°C-months) heat stress event during the 1997–1998 El Niño, with a larger response in the Wolf core. However, removing data that covers the 1997–1998 El Niño from calibration does not improve reconstruction statistics. Nevertheless, we find that excluding data *after* the 1997–1998 El Niño event from the calibration reduces the SST reconstruction error slightly. These results confirm that coral Sr/Ca is a reliable SST proxy in this region, although it can respond adversely to unusual heat stress. We suggest that noise in Sr/Ca-SST calibrations may be reduced by removing data immediately following large heat extremes.

Plain Language Summary The ratio of strontium to calcium (Sr/Ca) in reef-building coral skeletons has long been recognized to covary with the seawater temperature in which the corals grew and has been measured in many corals to understand past temperature changes. However, there are few examples from the eastern equatorial Pacific, an important region that drives variations in the climate system. Furthermore, this ratio might not reflect temperature as reliably after a heat stress event because of the physiological impacts on calcification processes. To test if Sr/Ca in corals from this region can reflect past temperature reliably and if this coral "thermometer" is compromised by heat stress, we analyze two coral records from the northern Galápagos. We find that Sr/Ca in these corals reflect temperature, but their relationship is weaker following heat stress and during the 21st century portion of our coral records. Although the heat stress event itself does not affect how well we can infer past temperature, using data after the event to establish the Sr/Ca-temperature relationship impacts the accuracy of temperature reconstruction. Our results demonstrate that excluding post-heat stress periods from the intervals during which these chemistry-climate relationships are developed may reduce the uncertainty of the resulting temperature reconstructions.

1. Introduction

Paleoclimate records based on the geochemistry of reef-building coral skeletons are critical for understanding tropical Pacific climate variability. The increasing number of coral geochemical records and synthesis studies in recent decades have improved our understanding of unforced and forced sea surface temperature (SST) variability in the tropical Pacific (e.g., Carilli et al., 2014; DeLong et al., 2007; Jimenez et al., 2018; Linsley et al., 2015; Nurhati et al., 2009; Tierney et al., 2015; Wu et al., 2014).

Despite these advancements, the spatiotemporal coverage of coral records remains extremely sparse, particularly in the eastern equatorial Pacific where marginal conditions and strong variability limit coral growth (Cole & Tudhope, 2017). Recent analyses have suggested the relationship between coral geochemistry and SST can be disrupted under extreme environmental conditions such as marine heatwaves (Clarke et al., 2017; 2019; D'Olivo & McCulloch, 2017; D'Olivo et al., 2019; Hetzinger et al., 2016; Leupold et al., 2019; Sagar et al., 2016), which

raises the question of the fidelity of these proxy records in capturing extreme conditions. Such limitations in data coverage and proxy uncertainties can hinder our ability to understand SST variability in the tropical Pacific (Comboul et al., 2015; Loope et al., 2020). To assess these challenges and the potential for long SST reconstructions from marginal reef environments in the eastern equatorial Pacific, we evaluate the impact of environmental stress on coral Sr/Ca calibration in the northern Galápagos.

Coral Sr/Ca is commonly used to reconstruct SST, based on a robust negative relationship between coral Sr/Ca and SST (hereafter "Sr/Ca-SST relationship") across many locations (e.g., Corrège, 2006 and references therein). This temperature dependence is also supported by aragonite precipitation experiments (DeCarlo et al., 2015; Gaetani & Cohen, 2006). However, the sensitivity of Sr/Ca to SST, as indicated by the linear regression slope, often differs among coral colonies (Alpert et al., 2016; DeLong et al., 2007; Grove et al., 2013; Sayani et al., 2019; Wu et al., 2014). This makes coral-based SST reconstruction difficult when empirical calibration is not possible (e.g., when using fossil corals for reconstruction). These disparities might partially arise from differences in laboratory and/or data processing methods, for instance sampling a suboptimal growth track or failing to properly account for observational uncertainties in the calibration (Alibert & McCulloch, 1997; DeLong et al., 2013; Reed et al., 2021; Wu et al., 2014).

Physiological processes may also impact the fidelity of the Sr/Ca-SST proxy (e.g., Allison & Finch, 2004; Goodkin et al., 2005; Thompson, 2021). Corals calcify from a fluid within a semi-enclosed environment (calcifying fluid) (Cohen & McConnaughey, 2003; Cohen & Gaetani, 2010), and preferentially incorporate or exclude trace elements (TEs) depending on their partition coefficients (K_D) (as reviewed by Thompson, 2021). For example, Sr incorporation is weakly favored in the skeleton (K_D Sr/Ca ~1.1) whereas Mg is strongly excluded (K_D Mg/Ca ~0.001). As calcification proceeds, therefore, the TE/Ca ratio in the calcifying fluid represents a balance between calcification and replenishment by ambient seawater through both active and passive transport processes (McCulloch et al., 2017; Sevilgen et al., 2019; Thompson, 2021). Changes in calcification rate can thus alter the geochemical composition of the calcifying fluid and the TE/Ca of the coral skeleton via Rayleigh fractionation (Cohen & Gaetani, 2010; Thompson, 2021). In addition, coral calcifying fluid geochemistry (and thus calcification) is also governed by active transcellular (i.e., through cells) and/or paracellular (i.e., between cells) pathways (Allemand et al., 2011; Thompson, 2021). In particular, active Ca^{2+} pumping (via the Ca-ATPase pump) incorporates Ca^{2+} (and Sr^{2+} as a by-product, Marchitto et al., 2018) and elevates pH of the calcifying fluid to maintain aragonite supersaturation of the calcifying fluid (Cohen & McConnaughey, 2003; Thompson, 2021).

Both Rayleigh fractionation and Ca^{2+} active transport affect the ratios of TEs to Ca in the calcifying fluid, and therefore the TE/Ca ratios in coral skeletons (Cohen & Gaetani, 2010; DeCarlo et al., 2015; Gaetani & Cohen, 2006). The strong statistical relationship between Sr/Ca and SST across numerous sites highlights that in most cases, these processes do not significantly impact Sr/Ca-based SST reconstructions. However, stressful environmental conditions may perturb the normal functioning of the coral's calcification physiology, for instance by disrupting metabolic and calcification processes, and create skeletal geochemical anomalies. Here we leverage unusually warm SST in Galápagos during an extreme El Niño event to document the impact of warming on the coral Sr/Ca-SST relationship.

The effects of temperature changes on coral calcification have been widely investigated. Past studies have documented that increases in average and extreme SSTs can cause the expulsion of zooxanthellae and coral bleaching (e.g., Hoegh-Guldberg, 1999). This has been observed in field surveys (Glynn, 1988; Glynn et al., 2015, 2018) and naturally extreme environments (Camp et al., 2018; Hoadley et al., 2019), and is further supported by growth rate measurements and stress bands in cores from massive corals (e.g., Barkley et al., 2018; DeCarlo & Cohen, 2017; Lough & Cantin, 2014). However, corals might be more resilient to temperature changes than previously thought. Geochemical and skeletal density analyses of cores from massive corals have suggested acclimatization to heat stress (Carilli et al., 2012; Clarke et al., 2019; DeCarlo et al., 2019; D'Olivo et al., 2019; Leupold et al., 2019; Thompson & van Woesik, 2009). Nevertheless, the relevant mechanisms remain disputed, and may include changes in genetics, the metabolic conditions, or the community of coral-associated microbes, including symbionts (e.g., Gibbin et al., 2018; Jones & Berkelmans, 2010; Palumbi et al., 2014; Ziegler et al., 2017). These studies provide multiple lines of evidence that changes in temperature can impact coral calcification.

Changes in coral calcification rate can impact the Sr/Ca of the calcifying fluid and the skeleton independent of SST. These non-climatic effects have obvious implications for using skeletal Sr/Ca to reconstruct SST. For

example, mounting evidence suggests that stressful conditions may disrupt the Sr/Ca-SST relationship (Clarke et al., 2017; 2019; D'Olivo & McCulloch, 2017; D'Olivo et al., 2019; Hetzinger et al., 2016; Leupold et al., 2019; Sagar et al., 2016). Previous studies have targeted corals that experienced a known heat stress event and demonstrated that such stress weakens the Sr/Ca-SST relationship. This breakdown is temporary: the relationship is usually restored within a year, although in some cases the disruption of the Sr/Ca-SST relationship can last several years (D'Olivo et al., 2019). Multiple mechanisms have been put forth to explain the disruption of the Sr/Ca-SST relationship, including: (a) reduced coral extension, which smooths out the seasonal cycle immediately after the stress event (Barnes et al., 1995; Clarke et al., 2019; Gagan et al., 2012), (b) a reduction in active transport via transcellular (e.g., Ca-ATPase) or paracellular pathways due to energy limitations, which reduces aragonite saturation of the calcifying fluid (Marshall & McCulloch, 2002), and (c) a reduction in calcification rate, which leads to a Rayleigh fractionation response (Clarke et al., 2017; D'Olivo & McCulloch, 2017; D'Olivo et al., 2019).

Despite evidence that heat stress can disrupt the Sr/Ca-SST relationship, we lack a clear mechanistic understanding of how this breakdown occurs and its impact on the fidelity of the resulting SST reconstruction. First, most prior studies have focused on corals from regions with similar mean SST and small SST variations. However, a single coral genus' heat stress response can vary in magnitude from site to site. Notably, corals accustomed to greater natural SST variability have been shown to be less susceptible to heat stress (Carilli et al., 2012; Sully et al., 2019; Thompson & van Woesik, 2009), and may therefore exhibit more consistent SST-TE/Ca relationships. Second, though evidence suggests the impacts of heat stress on the Sr/Ca-SST relationship can continue for several years (D'Olivo et al., 2019), most prior studies have only examined changes in the Sr/Ca-SST relationship during and immediately after a heat stress event. Thus, the statistics of the Sr/Ca-based SST reconstruction could be biased for some unknown period following temperature extremes. Third, the impacts of a disrupted Sr/Ca-SST relationship on Sr/Ca calibration and SST reconstruction have not been fully explored. Given that recent decades have been characterized by an increase in the frequency and intensity of heat stress (Fröhlicher et al., 2018; Hobday et al., 2016; Oliver et al., 2018), this disruption may have biased the Sr/Ca-SST calibrations used to reconstruct the history of SST and related phenomena (e.g., the El Niño-Southern Oscillation; ENSO). Altogether, these unknowns warrant further study to understand how the Sr/Ca-SST relationship may change in response to heat stress.

In this study, we present TE/Ca records measured in two modern *Porites lobata* corals collected from Wolf and Darwin Islands in the northern Galápagos archipelago, Ecuador, where large interannual SST variance, low pH, and high nutrients create marginal conditions for reef growth (Cortés, 1997; Cortés et al., 2017; Manzello et al., 2008). With these measurements, we address three overarching questions. First, at these marginal sites, does coral Sr/Ca exhibit a relationship with SST that is consistent with previous studies? Second, do heat stress events affect the relationship between Sr/Ca and SST at these sites? And third, if so, does excluding anomalous intervals improve SST reconstruction?

2. Materials and Methods

2.1. Eastern Equatorial Pacific and Galápagos Oceanography

The Galápagos archipelago lies along the equator, ~1000 km west of South America, in a region of large spatial and temporal environmental variability. A meridional SST gradient crosses the archipelago, with warmer conditions in the north and cooler in the south and west (Figure 1). Two major ocean currents govern the oceanography in the Galápagos: (a) the westward South Equatorial Current that splits into two lobes; and (b) the Equatorial Undercurrent that travels eastward in the subsurface and shoals when it strikes the Galápagos platform (Kessler, 2006).

Interannual ENSO extremes can significantly impact Galápagos corals. Both the high temperatures associated with El Niño events and the cooling during La Niñas cause stress and bleaching (Banks et al., 2009; Glynn et al., 2015, 2018). Virtually all coral colonies in the Galápagos archipelago experienced bleaching and mortality following the 1982-83 El Niño (Glynn, 1988); only colonies at Darwin and Wolf Islands showed significant regrowth after the event (Glynn et al., 2015). The 1997-8 El Nino event was also severe, triggering "island-wide" bleaching at Darwin (Glynn et al., 2015); Isla Wolf was not evaluated. Corals in the Galápagos archipelago also frequently experience multi-day rapid cooling events (~5–10°C) that are caused by thermocline shoaling (Banks et al., 2009; Riegl et al., 2019).

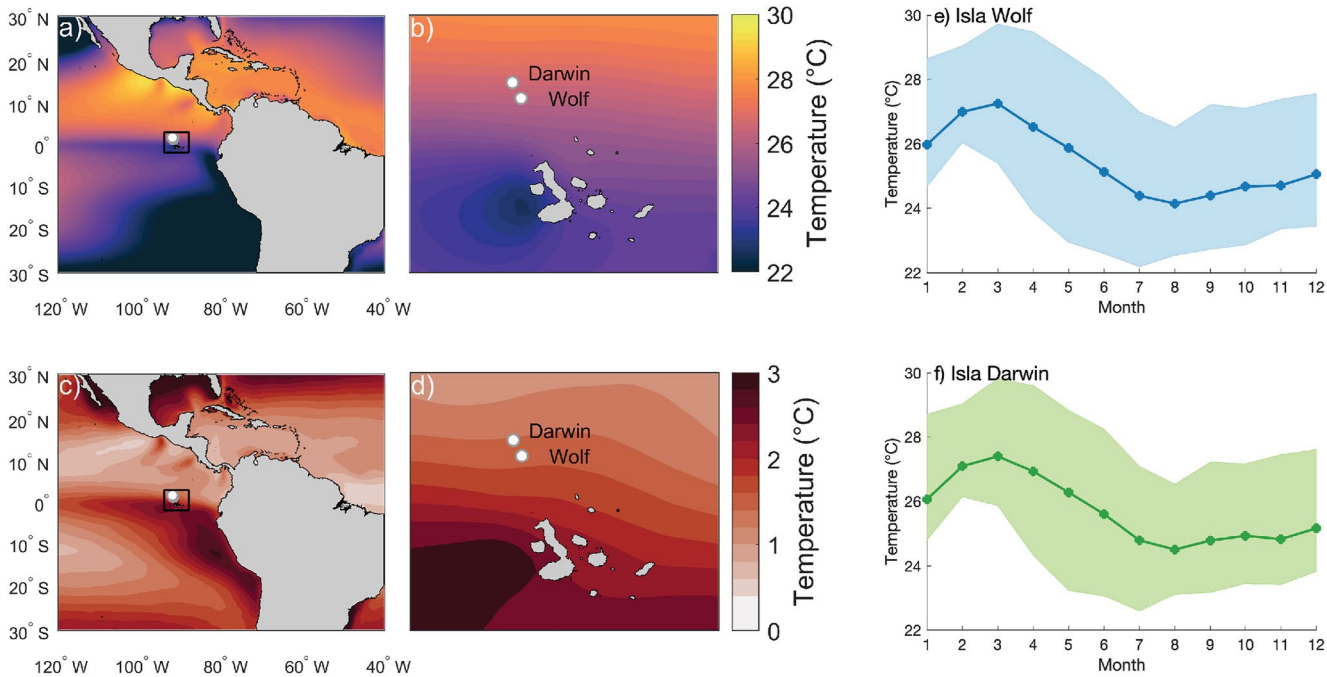

Figure 1. Site locations and climatology. (a–b) Mean annual sea surface temperature (SST) and (c–d) monthly SST standard deviation between 1982-2017 derived from OISST (Reynolds et al., 2007), where (b and d) represent areas enclosed by the boxes in (a and c). (e–f) SST climatology of Isla Wolf (GW10-10; blue) and Isla Darwin (GD15-3-1; green) with background color showing SST variations that cover the same span as the Sr/Ca records.

2.2. Coral Collection and Sampling

We analyzed coral cores from Isla Darwin (core GD15-3-1; 1°42' N, 92° W) and Isla Wolf (core GW10-10; 1°23'N, 91°50'W; Figure 1). Both cores were collected from living *P. lobata* coral using diver-operated hydraulic (Wolf) and pneumatic (Darwin) drills, in June 2010 at Wolf and in January 2015 at Darwin. In the lab, we halved, slabbed, and cleaned the cores by sonication in deionized water. Next, we x-rayed the slabs and used the resulting images to establish sampling transects along rapidly growing skeletal "fans" (Figure S1 in Supporting Information S1). We also examined two sections of GW10-10 and GD15-3-2 (different core from the same colony as GD15-3-1) with a scanning electron microscope to screen for diagenesis. Both sections showed pristine primary aragonite with no evidence of alteration (Figures S2–S3 in Supporting Information S1). We used an automated benchtop mill (Sherline Computer Numerical Control) to subsample the slabs at 1 mm resolution down core. Earlier measurements from the same powdered samples (GW10-10) were presented in Jimenez et al. (2018), although that study used a different ICP-OES instrument and associated methods and only focused on Sr/Ca.

2.3. Laboratory Methods

Our method was modified from Schrag (1999) and Cantarero et al. (2017). For each sample, 0.5–0.7 mg of coral powder was acidified with 3.5 mL of 5% trace metal grade HNO_3 to yield a solution of approximately 80 ppm Ca. We measured Sr (421 nm), Mg (285 nm), and Ca (315 nm) content with a radial torch view using a Thermo Electron Corporation iCap 7400 Inductively Coupled Plasma - Optimal Emission Spectrometer (ICP-OES) at the University of Arizona. We computed Sr/Ca and Mg/Ca elemental ratios using Sr (421 nm)/Ca (315 nm), and Mg (285 nm)/Ca (315 nm) output. We corrected the effects of plasma drift and matrix effects in these elemental ratios following Schrag (1999). To account for plasma drift, we measured a reference solution between each sample and adjusted the sample value. Next, in each run, we measured three matrix standards with same TE/Ca but with different Ca concentrations (60, 80, and 100 ppm) created by volumetric dilution of TE stock solutions; linear regression of measured TE/Ca values on Ca concentration in matrix standards was used to correct for matrix effects. Afterward, we normalized our data by adding the offset between a liquid internal coral standard (MCPL) measured independently at the University of Western Australia on an ICP-MS and average MCPL measured

value of each run. We also measured two internal coral powder standards (MCP and JCP-1) to estimate analytical uncertainty.

2.4. Age Model

To construct age models and calibrate our elemental records, we used the 0.25° × 0.25° monthly optimally interpolated sea surface temperature product version 2 (OISSTv2) (Reynolds et al., 2007). Prior to age modeling, we identified and removed geochemical outliers following Reed et al. (2021). To establish the age model for GW10-10 and GD15-3-1 elemental records, we identified each year's Sr/Ca minimum and tied it to the corresponding SST maximum (March) at grid cells 1.625°N, 267.875°E and 1.375°N, 268.125°E for GD15-3-1 and GW10-10, respectively. Finally, we linearly interpolated each elemental record to monthly time series based on the annual tie points.

2.5. Calibration and Residuals

We regressed the elemental records onto SST using weighted least squares (WLS) regression based on a maximum likelihood algorithm (Thirumalai et al., 2011; York et al., 2004) to identify the relationship between TE/Ca records and SST. WLS analysis accounts for uncertainty in both the SST and elemental time series and allows for correlation in errors. As such, it provides a more robust estimation of the SST-proxy relationship compared to ordinary least squares regression or reduced major axis regression (Thirumalai et al., 2011; York et al., 2004). We calculated the analytical uncertainty for each TE/Ca by taking 1 standard deviation (1σ) of the JCP-1 standard across all runs included in the data set ($n = 32$).

Following linear calibration, we analyzed the residuals from the Sr/Ca-SST regression to explore whether systematic behavior could be identified. If SST is sufficient to explain all systematic variations in Sr/Ca, then we expect the residuals to be independent and follow a normal distribution with zero mean. We determined whether (a) a linear trend was present in the residual using ordinary least squares regression, (b) the residuals were autocorrelated by analyzing the residuals' autocorrelation function, (c) the residuals were normally distributed through an Anderson-Darling test, and (d) the residuals scaled with observed SST. The significance of the trend and relationship between residual and observed SST were determined by analyzing the standard error of the regression. The significance of autocorrelation in the residuals was determined by calculating the large lag standard errors at lag k following Anderson (1976):

$$\sqrt{\mathrm{Var}(r_k)} \simeq \sqrt{\frac{1}{N}\left(1 + 2\sum_{i=1}^{K} r_i^2\right)} \tag{1}$$

where N = timeseries length, r_k = correlation at lag k.

2.6. Heat Stress Events

2.6.1. Definition

In Galápagos, heat stress events are commonly associated with strong El Niño conditions (Figure S4 in Supporting Information S1). We defined heat stress events from ERSST version 5 (Huang et al., 2017) using the Degrees Heat Month metric (DHM), calculated from a thermal stress threshold based on both the maximum climatological temperature and local temperature variability (Text S1 and Figure S5 in Supporting Information S1; Donner, 2011; Logan et al., 2012). Unlike Degree Heating Weeks (Liu et al., 2003), this approach enables us to use monthly SST data. We used ERSST because it covers a longer period, permitting a more rigorous assessment of baseline conditions; nevertheless, its spatial resolution is lower than OISST. As a result of this difference in temporal coverage and spatial resolution, the standard deviation of OISST data is larger by <2°C at both locations, and the mean value is slightly lower (Figure S6 in Supporting Information S1). The baseline condition (SST_c) over the climatological period was defined as:

$$SST_c = \langle \max(SST_i) \rangle \tag{2}$$

Following Donner (2011), the thermal threshold ($SST_{2.5\sigma}$) was defined as:

$$SST_{2.5\sigma} = 2.5 \times \sigma(\max(SST_i)) + SST_c \quad (3)$$

where $\max(SST_i)$ = maximum SST in year i, $\langle\rangle$ = average, σ = standard deviation. We defined the climatological period as 1950–1980; hence i = 1950, 1951, …, 1980. The DHM of a specific month is defined as the sum of temperature stress (in °C) exceeding this threshold ($SST_{2.5\sigma}$) during the current and preceding three months. We used Bleaching Alert thresholds defined in Donner (2011) to estimate the likelihood of bleaching due to heat stress: Bleaching Alert Level I threshold occurs at $2.5\sigma(\max(SST_i))°C$ ·month and Bleaching Alert Level II threshold occurs at $4.9\sigma(\max(SST_i))°C$ ·month. This approach is more robust than the traditional DHM definition because it takes into account the variable maximum SST in each year (Donner, 2011; Logan et al., 2012) and evidence that corals are less susceptible to extreme conditions when they experience large historical variability (Sully et al., 2019; Thompson & van Woesik, 2009). Previous work has also demonstrated improved bleaching predictability using this variability-based threshold over traditional DHM (Logan et al., 2012).

2.6.2. Regression and Jackknifing

We evaluated the impacts of heat stress events on Sr/Ca-SST relationships and SST reconstruction using three complementary approaches. First, we calculated running regressions between Sr/Ca and SST using 5 different moving windows to determine the temporal variability of the regression slope (2, 4, 6, 8, and 10 years). Second, we randomly removed varying lengths (1, 2, 4, 6, 8, and 10 years) of Sr/Ca and SST data, and used the remaining data to perform the regression. This allowed us to identify time periods and interval lengths that have the most significant impact on the regression slope. Third, we randomly removed 2 consecutive years of Sr/Ca and SST data to mimic the typical length of a heat stress event and split the remaining data into halves for calibration and reconstruction. Specifically, we developed the calibration equation using one half and applied the equation to the other half for reconstruction. We then compared the root mean square error (RMSE) between the reconstructed SST and instrumental SST. Since the RMSE is sensitive to both calibration and reconstruction, we also compared the RMSE using the other half for calibration/reconstruction. This allowed us to determine if including heat stress events in the calibration could influence the reconstruction skill.

2.6.3. Rayleigh Fractionation Model

To understand how calcification and active Ca^{2+} transport changed across the heat stress event, we modeled changes in TE/Ca using a closed system Rayleigh fractionation equation following Sinclair (2015):

$$\left(\frac{\mathrm{TE}}{\mathrm{Ca}}\right)_{arag} = \left(\frac{\mathrm{TE}}{\mathrm{Ca}}\right)_{cf} \frac{(1 - P^{K_{D_{TE}}})}{(1 - P)} \quad (4)$$

where $\left(\frac{\mathrm{TE}}{\mathrm{Ca}}\right)_{arag}$ is the TE/Ca ratio of the skeleton, $\left(\frac{\mathrm{TE}}{\mathrm{Ca}}\right)_{cf}$ is the TE/Ca ratio of the calcifying fluid, P is the proportion of Ca left in the calcifying fluid after precipitation has ended, and $K_{D_{TE}}$ is the partition coefficient of TE. Following D'Olivo and McCulloch (2017), we constructed two equations using Sr/Ca and Mg/Ca data and their respective K_D to solve for Ca_{cf} and P. K_D for Sr/Ca and Mg/Ca were calculated following $\mathrm{K_{DSr/Ca}} = \exp(-1.86 + 600/T_K)$ (Sinclair, 2015) and $\mathrm{K_{DMg/Ca}} = \exp(-13.13 + 1770/T_K)$ respectively. Calculations for $\mathrm{K_{DMg/Ca}}$ were modified slightly from Sinclair (2015), where $\mathrm{K_{DMg/Ca}} = \exp(-12.9 + 1860/T_K)$, so that P is constrained between 0 and 1 and $\mathrm{Ca_{cf}}$ is higher than seawater (>10.25 mmol/mol).

2.7. Age Model Sensitivity Test

We tested the sensitivity of our results to assumptions made in our age model. Our age modeling approach assumed that the growth rate was constant between each tie point and that maximum SST occurred in March. These assumptions introduce subannual uncertainties in our SST reconstruction and can bias the estimated variance (Lawman et al., 2020). Thus, we introduced two alternate age models to test the robustness of our results: one that tied Sr/Ca minima to observed (not climatological) maximum OISST SST of each year, and one that tied Sr/Ca maxima and minima to the observed minimum and maximum OISST SST of each year. These two alternate age models explore the impact of subannual age model uncertainties stemming from variations in the month when maximum SSTs occur each year and the variable seasonal growth rate (explored further in Reed et al. (2021) and Wellington and Glynn (1983); Text S2 in Supporting Information S1).

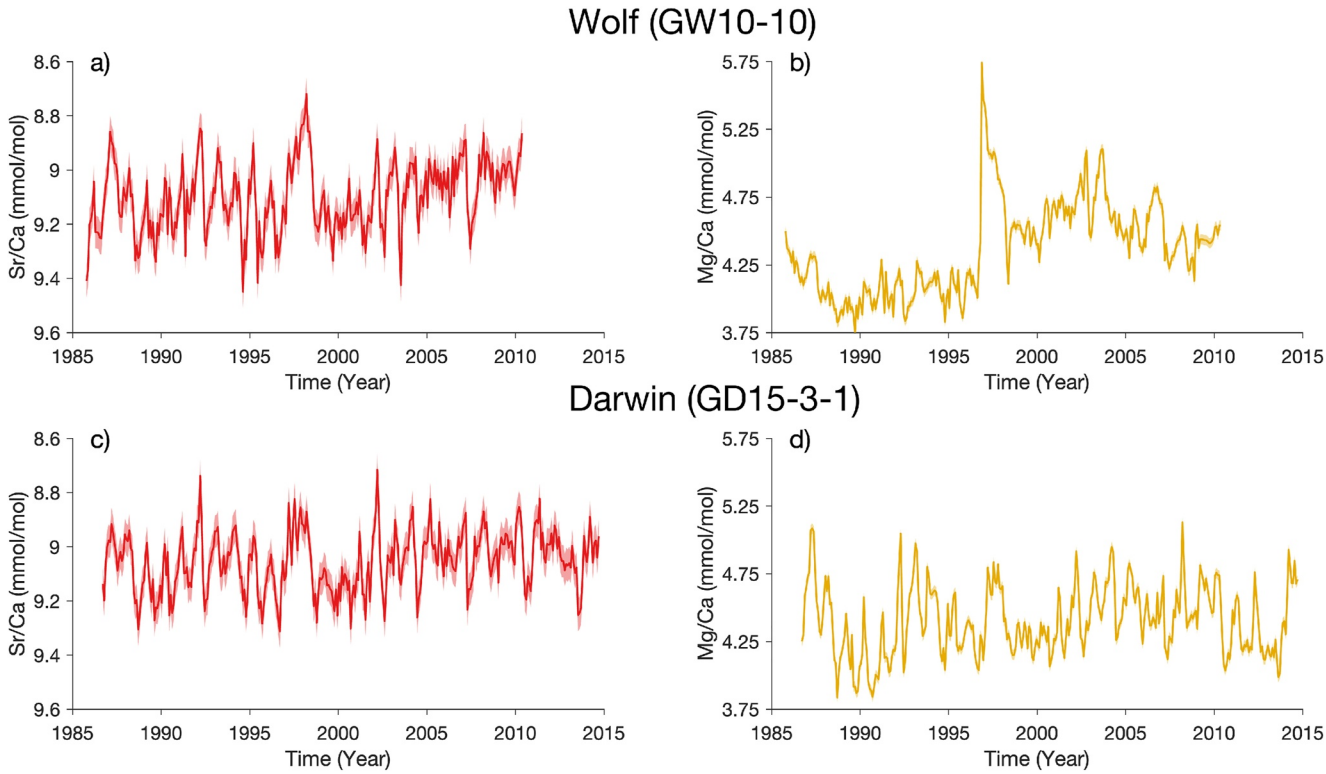

Figure 2. Time series of coral records. (a) Sr/Ca and (b) Mg/Ca time series from GW10-10. (c) Sr/Ca and (d) Mg/Ca time series from GD15-3-1. Lighter shaded background indicates 1σ analytical uncertainty.

3. Results and Discussion

The record from GW10-10 spans October 1985 to May 2010, and that from GD15-3-1 covers September 1986 to September 2014 (Figure 2). The mean values of Sr/Ca and Mg/Ca are comparable between the two cores (GW10-10 Sr/Ca: 9.099 mmol/mol, GD15-3-1 Sr/Ca: 9.055 mmol/mol; GW10-10 Mg/Ca: 4.368 mmol/mol, GD15-3-1 Mg/Ca: 4.403 mmol/mol). The Sr/Ca of GW10-10 exhibits greater variability (standard deviation) than that in GD15-3-1 (GW10-10 Sr/Ca: 0.128 mmol/mol, GD15-3-1 Sr/Ca: 0.109 mmol/mol). Although the Mg/Ca standard deviation for GW10-10 is also greater than that of GD15-3-1 GW10-10 Mg/Ca: 0.340 mmol/mol, GD15-3-1 Mg/Ca: 0.256 mmol/mol), this results from a single large anomaly that punctuates much lower-variability periods (discussed below).

3.1. Regression and Residuals

WLS regression based on monthly data demonstrates a negative relationship between Sr/Ca and SST at both sites. The regression slopes are -0.0625 ± 0.0024 and -0.0530 ± 0.0024 mmol/mol/°C ($\pm$1 standard error) for GW10-10 and GD15-3-1, respectively. A similar relationship between Sr/Ca and SST results from ordinary least squares (OLS) regression (Figure S7 in Supporting Information S1).

Sr/Ca calibration of our two records indicate a robust relationship between Sr/Ca and SST. Although the regression slopes are different between the two records, they are within the range suggested in previous synthesis studies (Corrège, 2006) and a previously published Sr/Ca reconstruction from the Galápagos (Jimenez et al., 2018). These results give confidence that Sr/Ca is a reliable paleothermometer at this site (Cole & Tudhope, 2017; Schrag, 1999).

Residuals from the linear regression between Sr/Ca and SST can provide additional insight into how well monthly Sr/Ca variations are linearly related to SST and whether factors other than SST systematically influence coral Sr/Ca. We analyzed four properties of the residuals from the Sr/Ca-SST regression at both sites (Figures 3a–3d, Figures S8a–S8d in Supporting Information S1). The Anderson-Darling test indicates residuals from GW10-10

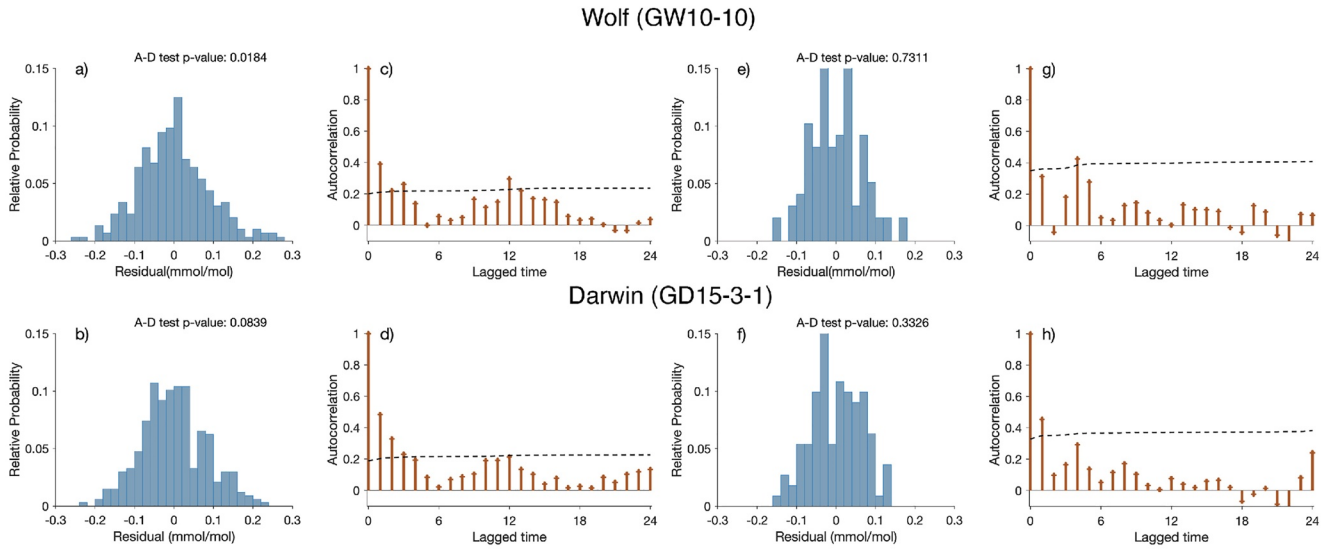

Figure 3. Residual characteristics from Sr/Ca calibration. Monthly data: (a–b) Residual distribution and (c–d) autocorrelation of residuals, with dashed line representing 2 standard error. Three-month averaged data: (e–f) Residual distribution, and (g–h) autocorrelation of residuals, with dashed line representing 2 standard error. Top row shows results from GW10-10 whereas bottom row shows results from GD15-3-1. Also shown are p-values of the Anderson Darling test.

exhibit non-normal behavior, whereas residuals from GD15-3-1 follow a normal distribution. The non-normal GW10-10 residual behavior is also reflected in higher order statistical moments (with a positively skewed, leptokurtotic distribution, Table 1). The skewness and kurtosis of GD15-3-1 residuals are closer to values expected from a normal distribution (Table 1). We also find significant autocorrelation in both residuals (up to 4 months lag). OLS regression of the Sr/Ca residuals as a function of time suggests residuals from both sites exhibit a statistically significant negative trend. Lastly, the amplitude of the Sr/Ca residual does not scale with observed SST, as indicated by the lack of significant correlation between the residuals and SST (Figures S8a–S8d in Supporting Information S1). The non-normal, autocorrelated residuals and the negative temporal trend in residuals violate the assumptions made in linear regression and suggest that not all systematic variations in Sr/Ca on monthly timescale are linearly related to SST.

Such non-normal behavior and autocorrelation in residuals could simply arise from errors in the age-depth model (Text S2 in Supporting Information S1) or the fact that a linear model cannot fully capture Sr/Ca-SST relationship. However, despite a strengthened Sr/Ca-SST relationship using the two alternate age models, the negative trend, the autocorrelation (in both cores), and the non-normal behavior (in GW10-10) of residuals persist (Figure S9 in Supporting Information S1). Furthermore, comparison between the goodness of fit of a linear, second order polynomial, and exponential models suggest that applying a higher order model to describe the Sr/Ca-SST relationship does not yield statistical benefit (not shown). These results imply that our assumptions related to age modeling (constant growth rate between tie points and stationary seasonality) and regression model are unlikely to be the only cause of autocorrelation and non-normal residuals, even though small (∼monthly) age offsets might systematically bias the Sr/Ca records on subseasonal timescales.

Table 1
Statistical Moments of GW10-10 and GD15-3-1 Sr/Ca-SST Residuals Using 1-Month and 3-Month Averaged Data

	GW10-10		GD15-3-1	
Moments	1 Month	3 Month	1 Month	3 Month
Mean	−5.9696E−6	−1.7219E−4	8.4963E−5	3.2586E−5
Variance	0.0081	0.0044	0.0066	0.0041
Skewness	0.3511	0.2124	0.1546	0.0246
Kurtosis	3.5637	2.9737	2.8910	2.4863

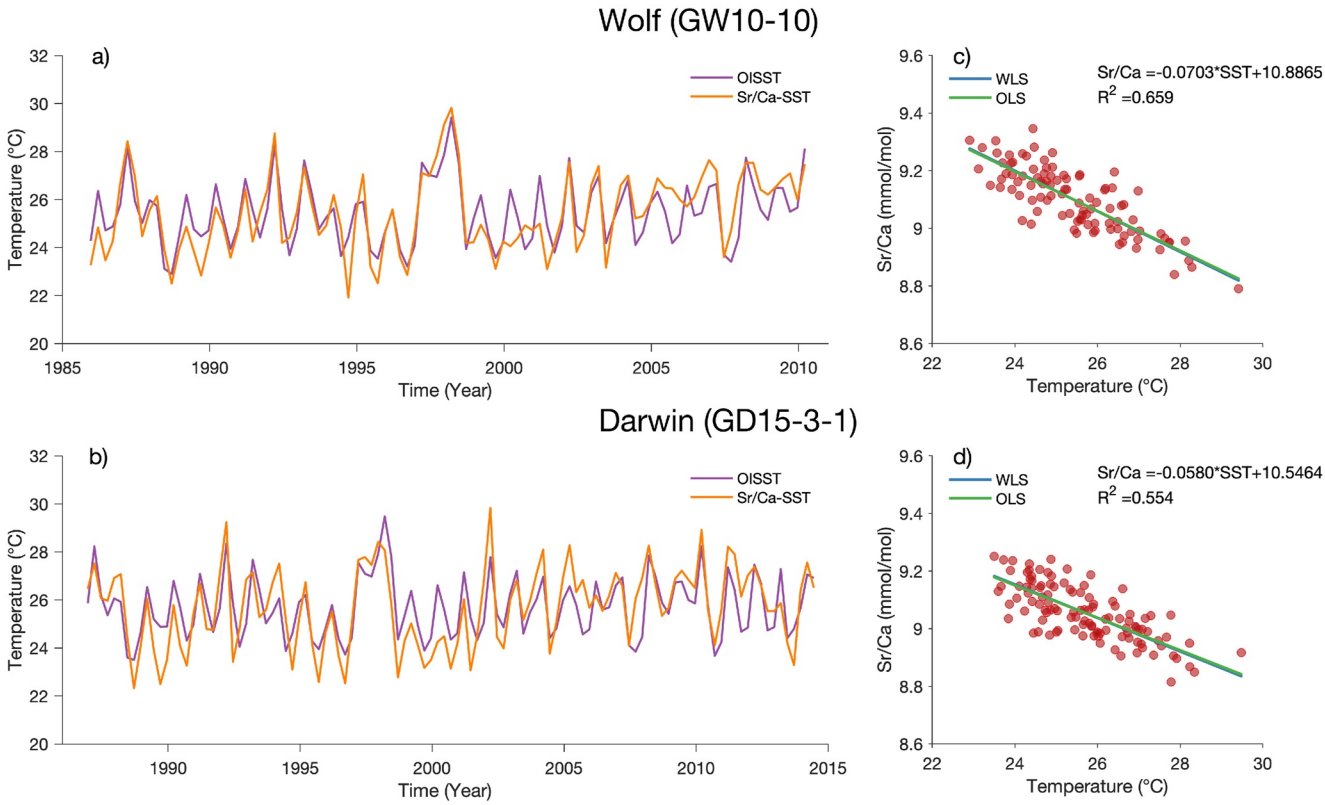

Figure 4. 3-month averaged Sr/Ca and sea surface temperature (SST) relationship. Time series of seasonal (February–April, May–July, August–October, November–January) instrumental SST and Sr/Ca-inferred SST from (a) GW10–10 and (b) GD15-3-1. Also shown are Sr/Ca regressed onto SST for (c) GW10–10 and (d) GD15-3-1 using a weight least square approach (WLS; blue) and ordinary least square approach (OLS; green).

To reduce the effects of subseasonal age uncertainty from our monthly resolution data, we create three-month ('seasonal') averages of Sr/Ca and SST centered on March, June, September, and December of each year. Next, we regress seasonal Sr/Ca onto seasonal SST for Sr/Ca calibration. This approach reduces autocorrelation in the residuals (Figures 3e–3h) while maintaining subannual resolution. In both cores, the Sr/Ca-SST correlation increases and the slope steepens compared to monthly resolution, with regression slopes of -0.0703 ± 0.0046 and -0.0580 ± 0.0046 mmol/mol/°C (± 1 standard error) for GW10-10 and GD15-3-1 respectively (Figure 4). This approach also reduces the skewness and kurtosis of residuals in GW10-10 and normalizes the distribution (Table 1). This result is consistent with the behavior of residuals in the monthly data set, where there is significant 1–4 months lagged correlation (Figure 3). Averaging monthly data to 3-month intervals thus minimizes the autocorrelation in the residual, and the 3-month regressions yield a more reliable estimate of the Sr/Ca-SST relationship. We present the remaining results based on the 3-month (seasonal) averaged data.

3.2. Heat Stress and Sr/Ca-SST Relationship

Based on the DHM metric, we identify three heat stress events since 1985 (Figure 5g), which correspond to well-known El Niño events (1987–1988, 1992–1993, and 1997–1998; Figure S4 in Supporting Information S1). The 1997–1998 event reached Bleaching Alert Level II, whereas 1987–1988 and 1992–1993 reached Bleaching Alert Level I. Comparing DHM to running regressions of Sr/Ca and SST, using varying running window lengths, we observe a weakened Sr/Ca-SST relationship after the 1997–1998 El Niño (Figure 5), when massive bleaching was recorded (Donner et al., 2017; Glynn, 2000). The reduction is particularly substantial in GW10-10. However, both cores capture the magnitude of the 1997–1998 El Niño event in their Sr/Ca records with remarkable consistency (Figure 4). Changes in Sr/Ca-SST relationship across the other Bleaching Alert I events are not apparent.

In contrast to Sr/Ca, Mg/Ca behaves differently in these cores, particularly across the 1997–1998 El Niño event. Prior to 1997, Mg/Ca correlates with Sr/Ca and with SST in both cores, but its range is much smaller in GW10-10

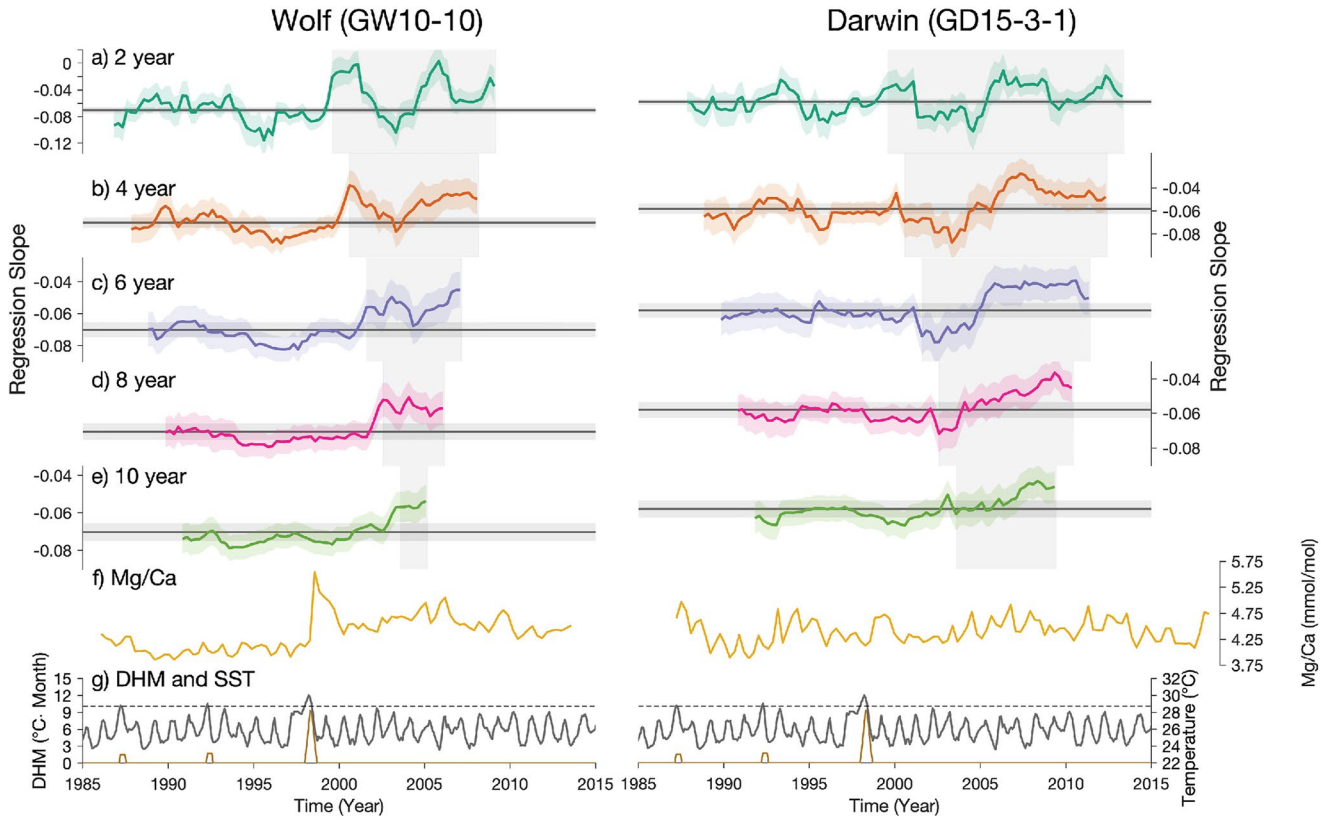

Figure 5. 3-month averaged running regression for GW10-10 (left) and GD15-3-1 (right). Regression slopes with (a) 2 years, (b) 4 years, (c) 6 years, (d) 8 years, (e) 10 years running window. Also shown are (f) Mg/Ca, (g) Degrees Heat Month (brown) and sea surface temperature (dark gray) with heat stress threshold (dashed line) for comparison. Black horizontal line and shadings shown in (a–e) represent the regression slope obtained using the full data set and 1σ weighted least squares uncertainty, respectively. Shaded area overlaid in each subplot represents periods post-1997 where the 1997–98 El Niño period was not included.

(Figure 7). In both cores, the initial warming in 1997 is accompanied by an anomalous increase in coral Mg/Ca; this is particularly notable in core GW10-10 (Figure 6). Following this event, we observe a sharp reduction in the Sr/Ca-SST relationship in the 2-year running regression window (Figure 5), as the Mg/Ca drops to a new baseline level of approximately 0.5 mmol/mol above pre-1997 values. In core GD15-3-1, we see a similar change in Mg/Ca ~1997; however, Mg/Ca returns to values that are comparable to pre-heat stress after the event, and the change in the Sr/Ca-SST relationship is smaller compared to GW10-10.

Other factors that could impact the Sr/Ca-SST relationship include irregular growth patterns that compromise optimal sampling strategy and reduced variance of SST that reduces signal/noise. The bottom section of GD15-3-1 was sampled in a region of irregular banding (Figure S1 in Supporting Information S1). However, we do not observe a shift in regression slope during that period (Figure 5). Moreover, the apparent stress response is weaker in the core with the more irregular growth (GD15-3-1), supporting the inference that suboptimal sampling does not play an important role in our results. We also note a reduction in standard deviation in SST and Sr/Ca after 1998, and during the early 1990s (Figure S10–S11 in Supporting Information S1). Critically, the weakened Sr/Ca-SST relationship only occurred post-1998. Hence, the weakened Sr/Ca-SST relationship cannot be explained either by suboptimal sampling of irregular growth or by a change in signal-to-noise ratio over time.

We therefore posit that coral physiological changes can explain the change in Sr/Ca-SST relationship following the 1997–1998 El Niño that caused regional bleaching. Previous studies have suggested three mechanisms that may weaken the Sr/Ca-SST relationship: a) attenuation of seasonality due to reduced extension rate and biosmoothing (Clarke et al., 2019; D'Olivo et al., 2019), b) reduced active ion transport (e.g., via Ca-ATPase pumping) due to diminished energy or DIC supply (Marshall & McCulloch, 2002), and c) a Rayleigh fractionation response to reduced calcification (Clarke et al., 2017; D'Olivo & McCulloch, 2017). Due to the contrasting

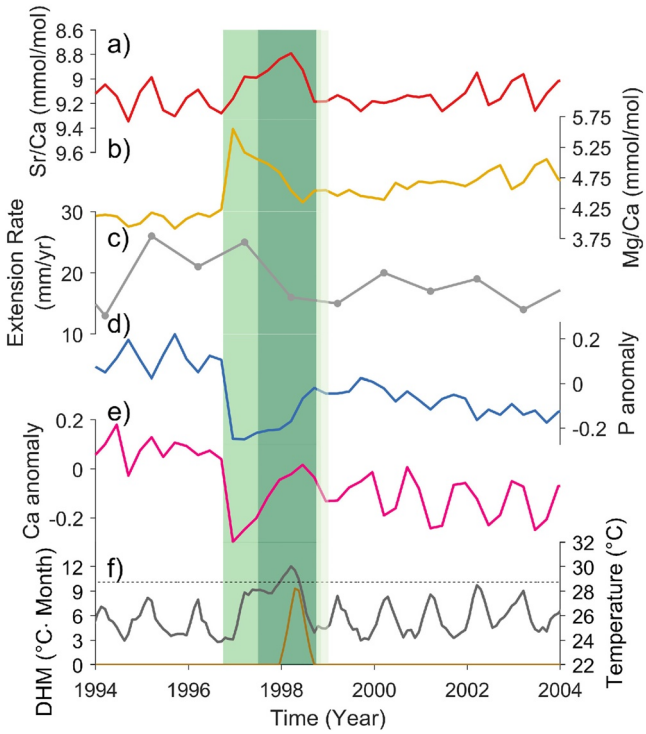

Figure 6. GW10-10 changes between 1994 and 2004. Variations of GW10-10 a) Sr/Ca, (b) Mg/Ca, (c) linear extension rate, (d) mean centered proportion of Ca^{2+} remaining in a batch of calcifying fluid after calcification finalizes (P) (e) mean centered concentration of Ca^{2+} in the calcifying fluid ($[Ca^{2+}]_{cf}$), and (f) SST conditions derived from ERSSTv5 between 1994 and 2004. The green shaded regions indicate the initial rise in Mg/Ca (green), accumulation of heat stress (dark green), and the return to 'normal' conditions (light green).

pathways by which each are impacted by heat stress, skeletal chemistry and growth changes can be used to distinguish among these mechanisms.

The simplest explanation is that under stress, coral extension slows, and the climate signal is not as finely sampled under a constant-depth, bulk sampling protocol, leading to undersampling the true variance (Barnes et al., 1995; D'Olivo et al., 2019; Gagan et al., 2012; Nothdurft & Webb, 2007). If this explanation were true, the seasonality of Sr/Ca and Mg/Ca would be reduced, but their relationship would not change. However, the relationship between seasonal Sr/Ca and Mg/Ca in GW10-10 changes dramatically after 1998 (Figure 7), indicating that biosmoothing cannot explain the weakening in Sr/Ca-SST correlation across the 1997–1998 heat stress event.

Alternatively, stress-related changes in active transport by paracellular or transcellular pathways (e.g., Ca-ATPase pumping) may explain the changes we observe. Both pathways require energy for ion transport, and may therefore be impacted by heat stress. However, they have contrasting impacts on TE/Ca ratios: transcellular pathways can concentrate ions against the electrochemical gradient, whereas paracellular pathways will equilibrate ions based on the concentration gradient between the calcifying fluid and seawater (as reviewed by Thompson, 2021). Evidence for elevated $[Ca^{2+}]$ in the calcifying fluid (DeCarlo et al., 2018; Sevilgen et al., 2019) suggests that the Ca-ATPase pump (a transcellular pathway) is important for ion transport, although the relative contribution of these pathways is still an active area of research. Using metabolic energy, Ca-ATPase actively pumps Ca^{2+} into the calcifying fluid for calcification. Concurrently, two H^+ are removed from the calcifying fluid, which elevates pH and aragonite saturation by shifting the carbonate reactions to favor $[CO_3]^{-2}$ (as reviewed by Thompson, 2021). Heat stress often causes corals to lose their symbiotic zooxanthellae (known as bleaching), which lowers the supply of energy available to power active Ca^{2+} transport (Marshall & McCulloch, 2002). The loss of metabolic energy would reduce the supply of Ca^{2+} to the calcifying fluid and decrease the calcifying fluid pH and aragonite saturation. This pump is thought to transport Sr similarly to Ca (Marchitto et al., 2018), but limited data suggest that it discriminates against Mg. Thus, a weakened Ca-ATPase pump would increase the Mg/Ca in the coral skeleton and leave Sr/Ca largely unchanged. Our Mg/Ca and Sr/Ca data during the heat stress interval are consistent with a weaker Ca-ATPase pump, especially in the Wolf core (Figure 6). Future work will utilize a suite of geochemical tracers, including boron isotope systematics, to assess changes in the pH and aragonite saturation of the coral calcifying fluid following thermal stress and bleaching.

Finally, changes in Rayleigh fractionation can also alter the Sr/Ca-SST relationship in corals. Rayleigh fractionation occurs due to the difference in partition coefficients among TEs, and leads to a negative relationship between Sr/Ca ($K_D \sim 1.1$) and Mg/Ca ($K_D \ll 1$) in the coral skeleton (amplified by the temperature dependence of Sr/Ca; Cohen & Gaetani, 2010; Marchitto et al., 2018; Thompson, 2021). Increased calcification rates would drive stronger Rayleigh partitioning, whereas reduced calcification would weaken it. If calcification slowed as a consequence of reduced Ca-ATPase pumping (i.e., driving calcification fluid toward lower aragonite saturation and lower pH), we would expect a lower Mg/Ca and higher Sr/Ca ratio as Rayleigh fractionation weakened (Cohen & Gaetani, 2010). We observe an anticorrelation between Mg/Ca and Sr/Ca in both cores prior to 1998, and a weakening/reversal of this relationship in GW10-10 only after 1998 (Figure 7). However, this weakened relationship is marked by an increase in Mg/Ca, which contradicts what would be expected from weakened Rayleigh fractionation. This result suggests that reduced Rayleigh fractionation alone cannot explain the unusual behavior of Sr/Ca and Mg/Ca in GW10-10.

In contrast with our results from Wolf, we see no significant change in the relationship between Sr/Ca and Mg/Ca before and after the heat stress event in the Darwin record. Changes in the post-event Sr/Ca-SST relationship are broadly similar to those at Wolf, but the Mg/Ca anomaly is smaller at Darwin. The reduction in Sr/Ca-SST relationship and changes in Sr/Ca and Mg/Ca could be a result of weakened Rayleigh fractionation at this site,

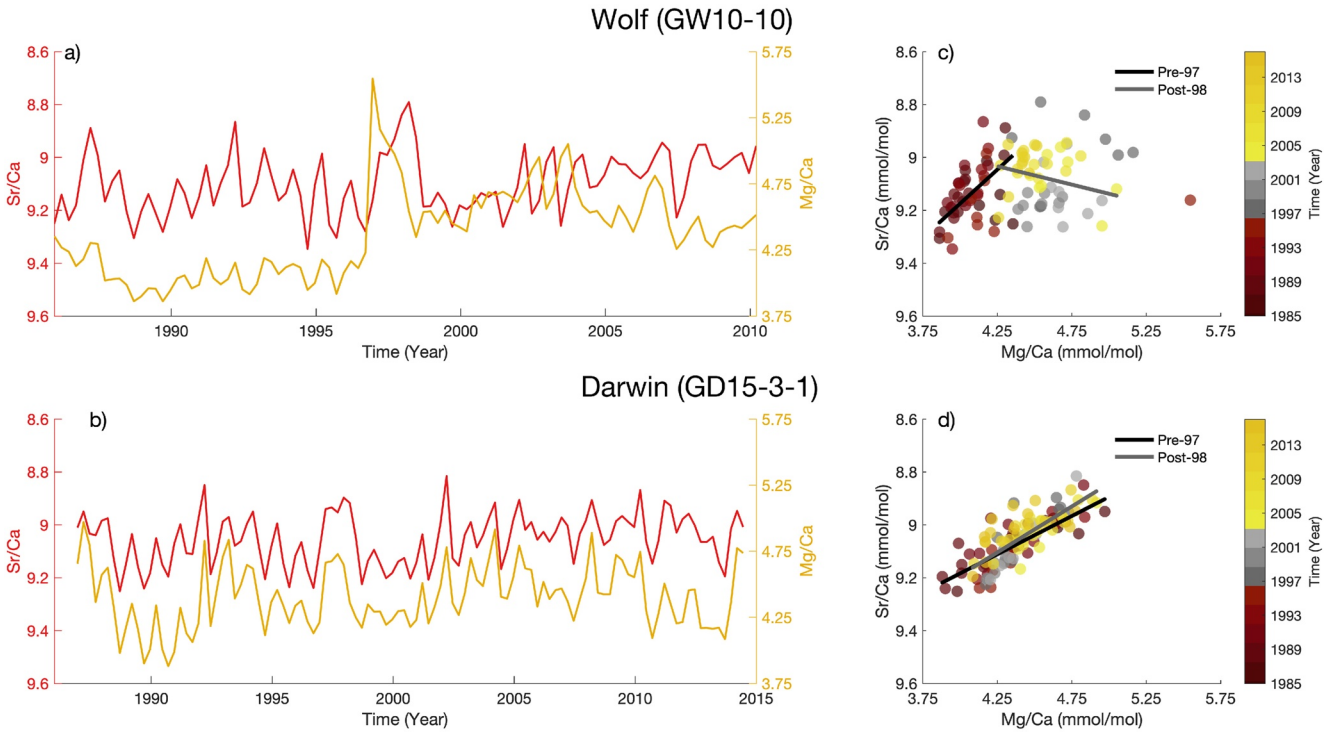

Figure 7. Sr/Ca and Mg/Ca relationship. (a–b) Time series of 3-month averaged Sr/Ca (red) and Mg/Ca (gold) and (c–d) scatter plot of Sr/Ca and Mg/Ca from GW10-10 (top) and GD15-3-1 (bottom). Color in scatter plots represents time as indicated by color bar. Also shown are regression lines calculating using data before 1997 (pre-97) and data after 1998 (post-98). Note that the *y*-axis of Sr/Ca is reversed.

but the smaller Mg/Ca anomaly and consistent relationship between Mg/Ca and Sr/Ca point to a reduced impact of heat on this coral.

Taking these results together, we argue that the short-term weakening of the Sr/Ca-SST relationship in the Wolf record is related to a reduction in available energy as bleaching cut off photosynthetic energy supplies. This energy loss weakened the Ca-ATPase pump, increasing Mg/Ca in the calcifying fluid and the skeleton (due to reduced Ca) and minimally impacting Sr/Ca (because both Sr and Ca are reduced). On the other hand, the slight weakening of the Sr/Ca-SST relationship and the lack of change in Sr/Ca-Mg/Ca relationship in the Darwin record suggests that the effects of coral calcification on the Sr/Ca-SST relationship were small in that colony. Regardless of the dominant mechanism(s), the small impact observed in GD15-3-1 suggests a stronger resilience to warming.

The difference in sensitivity to heat stress between these two corals is interesting. Although environmental variations could theoretically account for this difference, by influencing the amount of metabolic energy available and altering growth rate, in fact the islands are very similar in their climate; Wolf is cooler on average (~ 0.5°C) than Darwin (Riegl et al., 2019). Even at Wolf (i.e., within the same growth environment), the extension rates of different coral colonies vary substantially by (~1 cm/yr; Jimenez et al., 2018; Reed et al., 2021). These facts imply that environmental differences do not govern the growth rate and thus the sensitivity to heat stress. We suggest instead that colony-specific factors are more likely to be responsible for this difference. For example, symbiont taxa have different tolerances for temperature change, and the dominant symbiont type can affect corals' growth rate. If GW10-10 had a more sensitive symbiont type than GD15-3-1, it could have had a higher growth rate while also experiencing a more substantial loss of the energy powering the Ca-ATPase pump when under heat stress (Jones & Berkelmans, 2010). The intercolony difference in geochemistry suggests a greater sensitivity to heat stress in the Wolf colony, for example, bleaching or bleaching severity, compared to the one from Darwin.

3.3. Implications for Sr/Ca-SST Calibration

Many paleoclimate studies, including this one, rely on the recent SST record for calibration, when observations are most reliable, but also when heat stress events have been more frequent and intense (Oliver et al., 2018).

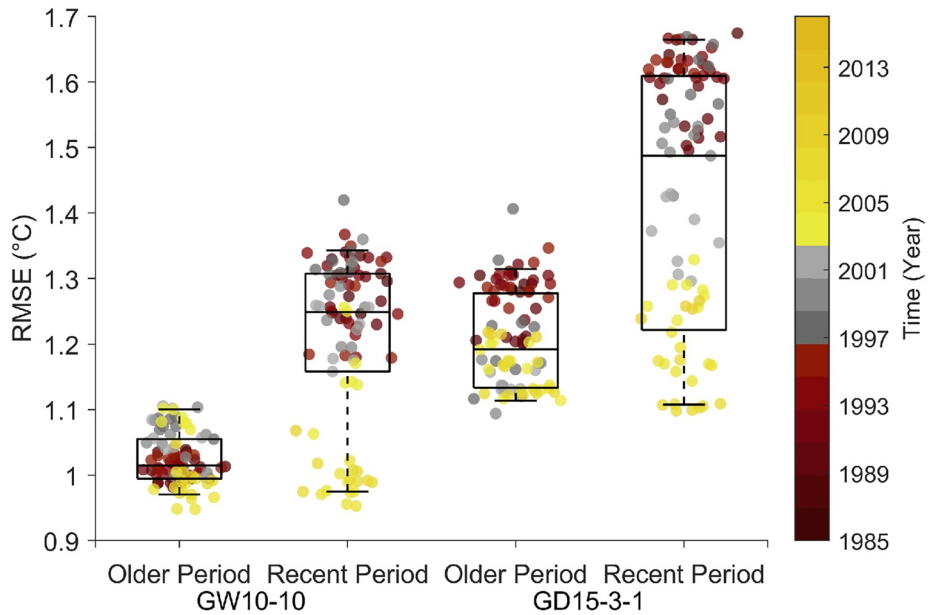

Figure 8. RMSE of reconstructed SST. RMSE of reconstructed SST after 2 years of data was removed from GW10-10 and GD15-3-1. The *x*-axis labels indicate which portion of the data was used for calibration (older: before the removed interval vs. recent: after the removed interval). Box and whiskers represent the reconstruction skill (RMSE). The color of the circles indicates the 2 years interval removed before calibration and reconstruction. The RMSE is centered on where the 2 years of data was removed.

Since our results suggest that heat stress impacts the relationship between Sr/Ca and SST, it is important to determine whether including heat stress events in the calibration can bias the Sr/Ca-SST relationship used for SST reconstruction.

We quantify the effect of heat stress events on the skill of the reconstruction. Removing 2 years of Sr/Ca-SST data across the 1997–1998 El Niño from the calibration period does not substantially change the reconstruction skill, as indicated by the RMSE (Figure 8). However, the reconstruction skill increases when excluding data following the heat stress event to establish calibration. This result is further corroborated by a more negative regression slope (i.e., a stronger SST dependence) when data near and after the largest heat stress event (1997-98 El Niño) are excluded from calculation (Figure S12 in Supporting Information S1).

Surprisingly, removing only heat stress events from the calibration data set does not significantly improve SST reconstruction. Nevertheless, the RMSE is higher when the more recent part of the data set is used for calibration, hinting at a long-term shift in the Sr/Ca-SST relationship in both records (Figure 8). Even though the underlying cause of this shift cannot be addressed with the data in hand, the fact that these patterns coincide with the 1997-98 El Niño suggest this shift might be a long-term response to heat stress. We note that the limited length of our data sets (~25 years) undermines our ability to fully quantify the uncertainty that this post heat stress response would add to a longer SST reconstruction. Nonetheless, our data suggest the choice of calibration could result in a ~0.3°C average difference in reconstruction.

4. Summary and Conclusion

Using seasonal data, we demonstrate that the Sr/Ca-SST relationship in these Galápagos corals is consistent with studies from other regions. We find that a large heat stress (strong El Niño) event affected the Sr/Ca-SST relationship in one of our two colonies. We attribute this change to a loss of metabolic energy from photosynthesis during a time of bleaching, resulting in weakening of the Ca-ATPase pump; we cannot rule out a secondary, minor attenuation of Rayleigh fractionation. Despite the impacts on the Sr/Ca-SST relationship, we do not find a significant increase in reconstruction error even when including this heat stress period. However, we show an

improvement in reconstruction skill when excluding the most recent (post-stress) data from calibration, highlighting the sensitivity of the reconstruction to the calibration data set.

Our study has three major implications. First, despite the tendency to calibrate Sr/Ca with SST at monthly resolution given a sufficient coral growth rate, our analyses suggest that this monthly relationship results in larger, non-climate-related residuals. Instead, using 3-month averaged data for Sr/Ca-SST calibration yields improved (Gaussian) residuals. We recommend routine examination of residuals when calibrating proxy to instrumental data. Second, the Sr/Ca-SST relationship in these corals is affected by heat stress, even in highly variable environments such as the eastern equatorial Pacific; the sensitivity varies among individuals. Lastly, although removing the heat stress period does not improve SST reconstruction, the SST reconstruction skill increases when data from the post-stress period is excluded from calibration, which could reflect a systemic response to heat stress. These results imply that calibrating Sr/Ca-SST using the most recent period, when corals have experienced greater levels of extreme heat stress, might increase SST reconstruction error. We suggest that calibration to instrumental data include analysis of the suitability of calibration intervals, not just in terms of instrumental data coverage, but also to exclude extreme events that might bias the calibration and resulting climate reconstruction.

Data Availability Statement

All data produced in this study are accessible at the National Center for Environmental Information paleoclimatology database at https://www.ncdc.noaa.gov/paleo/study/33894. The NOAA Physical Sciences Research Lab (Boulder, CO) provided ERSST V5 data (https://psl.noaa.gov/data/gridded/data.noaa.ersst.v5.html), and NOAA High Resolution SST data were accessed at https://climexp.knmi.nl/select.cgi?id=someone@somewhere&field=sstoiv2_monthly_mean.

Acknowledgments
The authors are grateful to the Parque Nacional Galápagos for permission and support to work in this very special place, and to the Charles Darwin Research Station for facilitating this project. Field sampling was enabled by the crew of the Queen Mabel and her captain Eduardo Rosero. Roberto Pepolas particularly improved our local understanding, coring efficiency, and safety over multiple field seasons. The authors also thank Jenifer Suarez, Meriwether Wilson, Diego Ruiz, Colin Chilcott, Jorge Baque, and Stephan Hlohowskyj for tireless field assistance and expertise. The authors thank Corey Shaver for her help in laboratory analysis, Emma Reed and Kelsey Dyez for helpful comments and suggestions, and Juan Pablo D'Olivo for the Rayleigh fractionation equation MATLAB code. This work was supported by NSF grants 1401326/1829613 and 0957881 to JEC, and by the University of Arizona Honors College Alumni Legacy Grant (Honors Thesis) and Brown University Presidential Fellowship to AHC. This publication is contribution #2415 of the Charles Darwin Foundation for the Galápagos Islands.

References

Alibert, C., & McCulloch, M. T. (1997). Strontium/calcium ratios in modern Porites corals from the Great Barrier Reef as a proxy for sea surface temperature: Calibration of the thermometer and monitoring of ENSO. *Paleoceanography*, *12*(3), 345–363. https://doi.org/10.1029/97PA00318

Allemand, D., Tambutté, É., Zoccola, D., & Tambutté, S. (2011). Coral calcification, cells to reefs. *Coral Reefs: An ecosystem in transition*, 119–150. https://doi.org/10.1007/978-94-007-0114-4_9

Allison, N., & Finch, A. A. (2004). High-resolution Sr/Ca records in modern Porites lobata corals: Effects of skeletal extension rate and architecture. *Geochemistry, Geophysics, Geosystems*, *5*(5). https://doi.org/10.1029/2004GC000696

Alpert, A. E., Cohen, A. L., Oppo, D. W., DeCarlo, T. M., Gove, J. M., & Young, C. W. (2016). Comparison of equatorial Pacific sea surface temperature variability and trends with Sr/Ca records from multiple corals. *Paleoceanography*, *31*(2), 252–265. https://doi.org/10.1002/2015PA002897

Anderson, O. D. (1976). *Time Series Analysis and Forecasting: The Box-Jenkins Approach* (Vol. 19). Butterworths London.

Banks, S., Vera, M., & Chiriboga, A. (2009). Establishing reference points to assess long-term change in zooxanthellate coral communities of the northern Galápagos coral reefs. *Galápagos Research*, *66*, 43–64.

Barkley, H. C., Cohen, A. L., Mollica, N. R., Brainard, R. E., Rivera, H. E., DeCarlo, T. M., et al. (2018). Repeat bleaching of a central Pacific coral reef over the past six decades (1960–2016). *Communications Biology*, *1*(1), 1–10. https://doi.org/10.1038/s42003-018-0183-7

Barnes, D., Taylor, R., & Lough, J. (1995). On the inclusion of trace materials into massive coral skeletons. Part II: Distortions in skeletal records of annual climate cycles due to growth processes. *Journal of Experimental Marine Biology and Ecology*, *194*(2), 251–275. https://doi.org/10.1016/0022-0981(95)00091-7

Camp, E. F., Schoepf, V., Mumby, P. J., Hardtke, L. A., Rodolfo-Metalpa, R., Smith, D. J., & Suggett, D. J. (2018). The future of coral reefs subject to rapid climate change: Lessons from natural extreme environments. *Frontiers in Marine Science*, *5*, 4. https://doi.org/10.3389/fmars.2018.00004

Cantarero, S. I., Tanzil, J. T. I., & Goodkin, N. F. (2017). Simultaneous analysis of Ba and Sr to Ca ratios in scleractinian corals by inductively coupled plasma optical emissions spectrometry. *Limnology and Oceanography: Methods*, *15*(1), 116–123. https://doi.org/10.1002/lom3.10152

Carilli, J. E., Donner, S. D., & Hartmann, A. C. (2012). Historical temperature variability affects coral response to heat stress. *PLoS One*, *7*(3), e34418. https://doi.org/10.1371/journal.pone.0034418

Carilli, J. E., McGregor, H. V., Gaudry, J. J., Donner, S. D., Gagan, M. K., Stevenson, S., et al. (2014). Equatorial Pacific coral geochemical records show recent weakening of the Walker circulation. *Paleoceanography*, *29*(11), 1031–1045. https://doi.org/10.1002/2014pa002683

Clarke, H., D'Olivo, J. P., Conde, M., Evans, R. D., & McCulloch, M. T. (2019). Coral records of variable stress impacts and possible acclimatization to recent marine heat wave events on the northwest shelf of Australia. *Paleoceanography and Paleoclimatology*, *34*(11), 1672–1688. https://doi.org/10.1029/2018PA003509

Clarke, H., D'Olivo, J. P., Falter, J., Zinke, J., Lowe, R., & McCulloch, M. (2017). Differential response of corals to regional mass-warming events as evident from skeletal Sr/Ca and Mg/Ca ratios. *Geochemistry, Geophysics, Geosystems*, *18*(5), 1794–1809. https://doi.org/10.1002/2016GC006788

Cohen, A., & Gaetani, G. A. (2010). Ion partitioning and the geochemistry of coral skeletons: Solving the mystery of the vital effect. *EMU Notes Mineral*, *11*, 377–397.

Cohen, A., & McConnaughey, T. (2003). Geochemical perspectives on coral mineralization. *Reviews in Mineralogy and Geochemistry*, *54*(1), 151–188. https://doi.org/10.1515/9781501509346-011

Cole, J., & Tudhope, A. W. (2017). Reef-based reconstructions of eastern Pacific climate variability. In P. W. Glynn, D. P. Manzello, & I. C. Enochs (Eds.), *Coral Reefs of the Eastern Tropical Pacific* (pp. 535–548). Springer. https://doi.org/10.1007/978-94-017-7499-4_19

Comboul, M., Emile-Geay, J., Hakim, G. J., & Evans, M. N. (2015). Paleoclimate sampling as a sensor placement problem. *Journal of Climate*, *28*(19), 7717–7740. https://doi.org/10.1175/JCLI-D-14-00802.1

Corrège, T. (2006). Sea surface temperature and salinity reconstruction from coral geochemical tracers. *Palaeogeography, Palaeoclimatology, Palaeoecology*, *232*(2–4), 408–428. https://doi.org/10.1016/j.palaeo.2005.10.014

Cortés, J. (1997). Biology and geology of eastern Pacific coral reefs. *Coral Reefs*, *16*(1), S39–S46. https://doi.org/10.1007/s003380050240

Cortés, J., Enochs, I. C., Sibaja-Cordero, J., Hernández, L., Alvarado, J. J., Breedy, O., et al. (2017). Marine biodiversity of eastern tropical Pacific coral reefs. In P. W. Glynn, D. P. Manzello, & I. C. Enochs (Eds.), *Coral reefs of the eastern tropical Pacific: Persistence and loss in a dynamic environment* (pp. 203–250): Springer Netherlands. https://doi.org/10.1007/978-94-017-7499-4_7

DeCarlo, T. M., & Cohen, A. L. (2017). Dissepiments, density bands and signatures of thermal stress in Porites skeletons. *Coral Reefs*, *36*(3), 749–761. https://doi.org/10.1007/s00338-017-1566-9

DeCarlo, T. M., Gaetani, G. A., Holcomb, M., & Cohen, A. L. (2015). Experimental determination of factors controlling U/Ca of aragonite precipitated from seawater: Implications for interpreting coral skeleton. *Geochimica et Cosmochimica Acta*, *162*, 151–165. https://doi.org/10.1016/j.gca.2015.04.016

DeCarlo, T. M., Harrison, H. B., Gajdzik, L., Alaguarda, D., Rodolfo-Metalpa, J., McCulloch, M. T., et al. (2019). Acclimatization of massive reef-building corals to consecutive heatwaves. *Proceedings of the Royal Society B: Biological Sciences*, *286*, 20190235. https://doi.org/10.1098/rspb.2019.0235

DeCarlo, T. M., Holcomb, M., & McCulloch, M. T. (2018). Reviews and syntheses: Revisiting the boron systematics of aragonite and their application to coral calcification. *Biogeosciences*, *15*(9), 2819–2834. https://doi.org/10.5194/bg-15-2819-2018

DeLong, K. L., Quinn, T. M., & Taylor, F. W. (2007). Reconstructing twentieth-century sea surface temperature variability in the southwest Pacific: A replication study using multiple coral Sr/Ca records from New Caledonia. *Paleoceanography*, *22*(4). https://doi.org/10.1029/2007PA001444

DeLong, K. L., Quinn, T. M., Taylor, F. W., Shen, C.-C., & Lin, K. (2013). Improving coral-base paleoclimate reconstructions by replicating 350 years of coral Sr/Ca variations. *Palaeogeography, Palaeoclimatology, Palaeoecology*, *373*, 6–24. https://doi.org/10.1016/j.palaeo.2012.08.019

D'Olivo, J. P., Georgiou, L., Falter, J., DeCarlo, T. M., Irigoien, X., Voolstra, C. R., et al. (2019). Long-term impacts of the 1997–1998 bleaching event on the growth and resilience of massive Porites corals from the central Red Sea. *Geochemistry, Geophysics, Geosystems*, *20*(6), 2936–2954. https://doi.org/10.1029/2019GC008312

D'Olivo, J. P., & McCulloch, M. (2017). Response of coral calcification and calcifying fluid composition to thermally induced bleaching stress. *Scientific Reports*, *7*(1), 1–15.

Donner, S. D. (2011). An evaluation of the effect of recent temperature variability on the prediction of coral bleaching events. *Ecological Applications*, *21*(5), 1718–1730. https://doi.org/10.1890/10-0107.1

Donner, S. D., Rickbeil, G. J., & Heron, S. F. (2017). A new, high-resolution global mass coral bleaching database. *PLoS One*, *12*(4). e0175490. https://doi.org/10.1371/journal.pone.0175490

Fröhlicher, T. L., Fischer, E. M., & Gruber, N. (2018). Marine heatwaves under global warming. *Nature*, *560*(7718), 360–364.

Gaetani, G. A., & Cohen, A. L. (2006). Element partitioning during precipitation of aragonite from seawater: A framework for understanding paleoproxies. *Geochimica et Cosmochimica Acta*, *70*(18), 4617–4634. https://doi.org/10.1016/j.gca.2006.07.008

Gagan, M. K., Dunbar, G. B., & Suzuki, A. (2012). The effect of skeletal mass accumulation in Porites on coral Sr/Ca and δ18O paleothermometry. *Paleoceanography*, *27*(1). https://doi.org/10.1029/2011PA002215

Gibbin, E. M., Krueger, T., Putnam, H. M., Barott, K. L., Bodin, J., Gates, R. D., & Meibom, A. (2018). Short-term thermal acclimation modifies the metabolic condition of the coral holobiont. *Frontiers in Marine Science*, *5*, 10. https://doi.org/10.3389/fmars.2018.00010

Glynn, P. W. (1988). El Niño—Southern Oscillation 1982–1983: Nearshore population, community, and ecosystem responses. *Annual Review of Ecology and Systematics*, *19*(1), 309–346. https://doi.org/10.1146/annurev.es.19.110188.001521

Glynn, P. W. (2000). Effects of the 1997–98 El Niño Southern Oscillation on eastern Pacific corals and coral reefs: An overview. *Proceeding of 9th International Coral Reef Symposium*, *2*, 1169–1174.

Glynn, P. W., Feingold, J. S., Baker, A., Banks, S., Baums, I. B., Cole, J., et al. (2018). State of corals and coral reefs of the Galápagos islands (Ecuador): Past, present and future. *Marine Pollution Bulletin*, *133*, 717–733. https://doi.org/10.1016/j.marpolbul.2018.06.002

Glynn, P. W., Riegl, B., Purkis, S., Kerr, J. M., & Smith, T. B. (2015). Coral reef recovery in the Galápagos islands: The northernmost islands (Darwin and Wenman). *Coral Reefs*, *34*(2), 421–436. https://doi.org/10.1007/s00338-015-1280-4

Goodkin, N. F., Hughen, K. A., Cohen, A. L., & Smith, S. R. (2005). Record of Little Ice Age sea surface temperatures at Bermuda using a growth-dependent calibration of coral Sr/Ca. *Paleoceanography*, *20*(4). https://doi.org/10.1029/2005PA001140

Grove, C. A., Kasper, S., Zinke, J., Pfeiffer, M., Garbe-Schönberg, D., & Brummer, G.-J. A. (2013). Confounding effects of coral growth and high SST variability on skeletal Sr/Ca: Implications for coral paleothermometry. *Geochemistry, Geophysics, Geosystems*, *14*(4), 1277–1293. https://doi.org/10.1002/ggge.20095

Hetzinger, S., Pfeiffer, M., Dullo, W.-C., Zinke, J., & Garbe-Schönberg, D. (2016). A change in coral extension rates and stable isotopes after El Niño-induced coral bleaching and regional stress events. *Scientific Reports*, *6*. https://doi.org/10.1038/srep32879

Hoadley, K. D., Lewis, A. M., Wham, D. C., Pettay, D. T., Grasso, C., Smith, R., & Warner, M. E. (2019). Host–symbiont combinations dictate the photo-physiological response of reef-building corals to thermal stress. *Scientific Reports*, *9*(1), 1–15. https://doi.org/10.1038/s41598-019-46412-4

Hobday, A. J., Alexander, L. V., Perkins, S. E., Smale, D. A., Straub, S. C., Oliver, E. C., et al. (2016). A hierarchical approach to defining marine heatwaves. *Progress in Oceanography*, *141*, 227–238. https://doi.org/10.1016/j.pocean.2015.12.014

Hoegh-Guldberg, O. (1999). Climate change, coral bleaching and the future of the world's coral reefs. *Marine and Freshwater Research*, *50*(8), 839–866. https://doi.org/10.1071/mf99078

Huang, B., Thorne, P. W., Banzon, V. F., Boyer, T., Chepurin, G., Lawrimore, J. H., et al. (2017). Extended Reconstructed Sea Surface Temperature, version 5 (ERSSTv5): Upgrades, validations, and intercomparisons. *Journal of Climate*, *30*(20), 8179–8205. https://doi.org/10.1175/JCLI-D-16-0836.1

Jimenez, G., Cole, J. E., Thompson, D. M., & Tudhope, A. W. (2018). Northern Galápagos corals reveal twentieth century warming in the eastern tropical Pacific. *Geophysical Research Letters*, *45*, 1981–1988. https://doi.org/10.1002/2017GL075323

Jones, A., & Berkelmans, R. (2010). Potential costs of acclimatization to a warmer climate: Growth of a reef coral with heat tolerant vs. sensitive symbiont types. *PLoS One*, *5*(5). e10437. https://doi.org/10.1371/journal.pone.0010437

Kessler, W. S. (2006). The circulation of the eastern tropical Pacific: A review. *Progress in Oceanography*, *69*(2–4), 181–217. https://doi.org/10.1016/j.pocean.2006.03.009

Lawman, A. E., Partin, J. W., Dee, S. G., Casadio, C. A., Di Nezio, P., & Quinn, T. M. (2020). Developing a coral proxy system model to compare coral and climate model estimates of changes in paleo-ENSO variability. *Paleoceanography and Paleoclimatology*, *35*(7). e2019PA003836. https://doi.org/10.1029/2019PA003836

Leupold, M., Pfeiffer, M., Garbe-Schönberg, D., & Sheppard, C. (2019). Reef-scale-dependent response of massive Porites corals from the Central Indian Ocean to prolonged thermal stress: Evidence from coral Sr/Ca measurements. *Geochemistry, Geophysics, Geosystems*, *20*(3), 1468–1484. https://doi.org/10.1029/2018GC007796

Linsley, B. K., Wu, H. C., Dassié, E. P., & Schrag, D. P. (2015). Decadal changes in south Pacific sea surface temperatures and the relationship to the Pacific decadal oscillation and upper ocean heat content. *Geophysical Research Letters*, *42*, 2358–2366. https://doi.org/10.1002/2015GL063045

Liu, G., Strong, A. E., & Skirving, W. (2003). Remote sensing of sea surface temperatures during 2002 barrier reef coral bleaching. *Eos, Transactions American Geophysical Union*, *84*(15), 137–141. https://doi.org/10.1029/2003eo150001

Logan, C. A., Dunne, J., Eakin, C., & , Donner, S. (2012). A framework for comparing coral bleaching thresholds. In Yellowlees, D., & Hughes, T. P. (Eds.), *Proceedings of the 12th International Coral Reef Symposium*. pp 10a3 townsville [internet].

Loope, G., Thompson, D., Cole, J., & Overpeck, J. (2020). Is there a low-frequency bias in multiproxy reconstructions of tropical Pacific SST variability? *Quaternary Science Reviews*, *246*. https://doi.org/10.1016/j.quascirev.2020.106530

Lough, J. M., & Cantin, N. E. (2014). Perspectives on massive coral growth rates in a changing ocean. *The Biological Bulletin*, *226*(3), 187–202. https://doi.org/10.1086/BBLv226n3p187

Manzello, D. P., Kleypas, J. A., Budd, D. A., Eakin, C. M., Glynn, P. W., & Langdon, C. (2008). Poorly cemented coral reefs of the eastern tropical Pacific: Possible insights into reef development in a high-CO2 world. *Proceedings of the National Academy of Sciences*, *105*(30), 10450–10455. https://doi.org/10.1073/pnas.0712167105

Marchitto, T., Bryan, S., Doss, W., McCulloch, M., & Montagna, P. (2018). A simple biomineralization model to explain Li, Mg, and Sr incorporation into aragonitic foraminifera and corals. *Earth and Planetary Science Letters*, *481*, 20–29. https://doi.org/10.1016/j.epsl.2017.10.022

Marshall, J. F., & McCulloch, M. T. (2002). An assessment of the Sr/Ca ratio in shallow water hermatypic corals as a proxy for sea surface temperature. *Geochimica et Cosmochimica Acta*, *66*(18), 3263–3280. https://doi.org/10.1016/s0016-7037(02)00926-2

McCulloch, M., D'Olivo, J. P., Falter, J., Holcomb, M., & Trotter, J. A. (2017). Coral calcification in a changing world and the interactive dynamics of pH and DIC upregulation. *Nature Communications*, *8*(1), 1–8. https://doi.org/10.1038/ncomms15686

Nothdurft, L. D., & Webb, G. E. (2007). Microstructure of common reef-building coral genera Acropora, Pocillopora, Goniastrea and Porites: Constraints on spatial resolution in geochemical sampling. *Facies*, *53*(1), 1–26. https://doi.org/10.1007/s10347-006-0090-0

Nurhati, I. S., Cobb, K. M., Charles, C. D., & Dunbar, R. B. (2009). Late 20th century warming and freshening in the central tropical Pacific. *Geophysical Research Letters*, *36*(21). https://doi.org/10.1029/2009GL040270

Oliver, E. C., Donat, M. G., Burrows, M. T., Moore, P. J., Smale, D. A., Alexander, L. V., et al. (2018). Longer and more frequent marine heatwaves over the past century. *Nature Communications*, *9*(1), 1–12. https://doi.org/10.1038/s41467-018-03732-9

Palumbi, S. R., Barshis, D. J., Traylor-Knowles, N., & Bay, R. A. (2014). Mechanisms of reef coral resistance to future climate change. *Science*, *344*(6186), 895–898. https://doi.org/10.1126/science.1251336

Reed, E. V., Thompson, D. M., Cole, J. E., Lough, J. M., Cantin, N. E., Cheung, A. H., et al. (2021). Impacts of coral growth on geochemistry: Lessons from the Galápagos islands. *Paleoceanography and Paleoclimatology*, *36*(4). e2020PA004051. https://doi.org/10.1029/2020PA004051

Reynolds, R. W., Smith, T. M., Liu, C., Chelton, D. B., Casey, K. S., & Schlax, M. G. (2007). Daily high-resolution-blended analyses for sea surface temperature. *Journal of Climate*, *20*(22), 5473–5496. https://doi.org/10.1175/2007JCLI1824.1

Riegl, B., Johnston, M., Glynn, P. W., Keith, I., Rivera, F., Vera-Zambrano, M., & Glynn, P. J. (2019). Some environmental and biological determinants of coral richness, resilience and reef building in Galápagos (Ecuador). *Scientific Reports*, *9*(1), 1–16. https://doi.org/10.1038/s41598-019-46607-9

Sagar, N., Hetzinger, S., Pfeiffer, M., Masood Ahmad, S., Dullo, W.-C., & Garbe-Schönberg, D. (2016). High-resolution Sr/Ca ratios in a Porites lutea coral from Lakshadweep archipelago, southeast Arabian sea: An example from a region experiencing steady rise in the reef temperature. *Journal of Geophysical Research: Oceans*, *121*, 252–266. https://doi.org/10.1002/2015JC010821

Sayani, H. R., Cobb, K. M., DeLong, K., Hitt, N. T., & Druffel, E. R. M. (2019). Intercolony δ18O and Sr/Ca variability among Porites spp. corals at Palmyra Atoll: Toward more robust coral-based estimates of climate. *Geochemistry, Geophysics, Geosystems*, *20*(11), 5270–5284. https://doi.org/10.1029/2019GC008420

Schrag, D. P. (1999). Rapid analysis of high-precision Sr/Ca ratios in corals and other marine carbonates. *Paleoceanography*, *14*(2), 97–102. https://doi.org/10.1029/1998PA900025

Sevilgen, D. S., Venn, A. A., Hu, M. Y., Tambutté, E., de Beer, D., Planas-Bielsa, V., & Tambutté, S. (2019). Full in vivo characterization of carbonate chemistry at the site of calcification in corals. *Science advances*, *5*(1). eaau7447. https://doi.org/10.1126/sciadv.aau7447

Sinclair, D. J. (2015). Rbme coral temperature reconstruction: An evaluation, modifications, and recommendations. *Geochimica et Cosmochimica Acta*, *154*, 66–80. https://doi.org/10.1016/j.gca.2015.01.006

Sully, S., Burkepile, D., Donovan, M., Hodgson, G., & Van Woesik, R. (2019). A global analysis of coral bleaching over the past two decades. *Nature Communications*, *10*(1), 1–5. https://doi.org/10.1038/s41467-019-09238-2

Thirumalai, K., Singh, A., & Ramesh, R. (2011). A Matlab™ code to perform weighted linear regression with (correlated or uncorrelated) errors in bivariate data. *Journal of the Geological Society of India*, *77*(4), 377–380. https://doi.org/10.1007/s12594-011-0044-1

Thompson, D. M. (2021). Environmental records from coral skeletons: A decade of novel insights and innovation. *WIRES Climate Change*. https://doi.org/10.1002/wcc.745

Thompson, D. M., & van Woesik, R. (2009). Corals escape bleaching in regions that recently and historically experienced frequent thermal stress. *Proceedings of the Royal Society B: Biological Sciences*, *276*(1669), 2893–2901. https://doi.org/10.1098/rspb.2009.0591

Tierney, J. E., Abram, N. J., Anchukaitis, K. J., Evans, M. N., Giry, C., Kilbourne, K. H., et al. (2015). Tropical sea surface temperatures for the past four centuries reconstructed from coral archives. *Paleoceanography*, *30*(3), 226–252. https://doi.org/10.1002/2014PA002717

Wellington, G. M., & Glynn, P. W. (1983). Environmental influences on skeletal banding in eastern Pacific (Panama) corals. *Coral Reefs*, *1*(4), 215–222. https://doi.org/10.1007/bf00304418

Wu, H. C., Moreau, M., Linsley, B. K., Schrag, D. P., & Corrège, T. (2014). Investigation of sea surface temperature changes from replicated coral Sr/Ca variations in the eastern equatorial Pacific (Clipperton Atoll) since 1874. *Palaeogeography, Palaeoclimatology, Palaeoecology*, *412*, 208–222. https://doi.org/10.1016/j.palaeo.2014.07.039

York, D., Evensen, N. M., Martınez, M. L., & De Basabe Delgado, J. (2004). Unified equations for the slope, intercept, and standard errors of the best straight line. *American Journal of Physics*, *72*(3), 367–375. https://doi.org/10.1119/1.1632486

Ziegler, M., Seneca, F. O., Yum, L. K., Palumbi, S. R., & Voolstra, C. R. (2017). Bacterial community dynamics are linked to patterns of coral heat tolerance. *Nature Communications*, *8*(1), 1–8. https://doi.org/10.1038/ncomms14213